Author Manuscript

Author Manuscript

Author Manuscript

Author Manuscript

HHS Public Access

Author manuscript

Protein Expr Purif. Author manuscript; available in PMC 2025 January 01.

Published in final edited form as:

Protein Expr Purif. 2024 January ; 213: 106362. doi:10.1016/j.pep.2023.106362.

Optimized expression and purification of a human adenosine deaminase in *E. coli* and characterization of its Asp8Asn variant

Maria Rain Jennings[1], **Soohyon Min**[1], **Grace S. Xu**[1], **Kassandra Homayuni**[1], **Bhavana Suresh**[1], **Yusef Amir Haikal**[1], **John Blazeck**[1,*]

[1]School of Chemical and Biomolecular Engineering, Georgia Institute of Technology, Atlanta GA 30332, USA.

Abstract

Homo sapiens adenosine deaminase isoform 1 (HsADA1) hydrolyzes adenosine and 2-deoxyadenosine as a key step in the purine nucleoside salvage pathway. Some HsADA1 mutations have severe deleterious effects, as is the case in a severe combined immunodeficiency resulting from loss of enzyme activity (ADA-SCID). Other mutations that reduce enzyme activity, for instance the Asp8Asn (D8N) variant, do not cause ADA-SCID but are correlated with other consequences to health. To ease further study of HsADA1 and its variants, we optimized an inexpensive, recombinant expression process in an *Escherichia coli* host through multiplexed parameter testing enabled by a lysate-based microtiter plate assay. We demonstrate the importance of gene codon usage, induction time and temperature, and alcohol supplementation towards improving enzyme yield to a final titer of 5 milligrams per liter of culture. We further show that use of a double-histidine-tag (his-tag) system greatly improves purity. We then utilize our expression and purification framework to produce the HsADA1 D8N variant, which had previously not been purified to homogeneity. We confirm that the D8N variant is ~30% less active than the wildtype HsADA1 and show that it better retains its activity in human serum. Additionally, we show that both HsADA1 and the D8N variant have heightened activity in serum, driven in part by a previously undescribed phenomenon involving albumin. Therefore, this work

*Corresponding author.

COMPETING INTERESTS

JB and MRJ have filed a patent application in relation to this work.

CRediT AUTHOR CONTRIBUTIONS

Conceptualization: JB, MRJ. Methodology: JB, MRJ. Formal analysis: MRJ. Investigation: MRJ, SM, GSX, KH, BS, YAH. Writing – original draft: MRJ. Writing – review & editing – MRJ, JB. Visualization: MRJ. Supervision: JB. Funding acquisition: JB.

Statements:

Author Statements:

All authors acknowledge the following four statements to be true:

1) All authors concur with the submission.

2) The work has not been published elsewhere, either completely, in part, or in another form. 3) The manuscript has not been submitted to another journal and will not be published elsewhere within one year after its publication in this journal.

4) The manuscript does not contain experiments using animals.

AI Statement:

N/A

Publisher's Disclaimer: This is a PDF file of an unedited manuscript that has been accepted for publication. As a service to our customers we are providing this early version of the manuscript. The manuscript will undergo copyediting, typesetting, and review of the resulting proof before it is published in its final form. Please note that during the production process errors may be discovered which could affect the content, and all legal disclaimers that apply to the journal pertain.

Author Manuscript Author Manuscript Author Manuscript Author Manuscript

presents a valuable process to produce HsADA1 that allows for insights into it and its variants' behavior. We also confirm the utility of lysate-based activity assays towards finding optimal *E. coli* expression conditions for enzymes and show how fusing his-tags in tandem can enhance product purity.

Keywords

adenosine deaminase; bacterial lysate screening; double-his-tag

INTRODUCTION

Adenosine deaminases (ADAs) are ubiquitously expressed within human tissues as key parts of the purine nucleoside salvage pathway [1]. The *Homo sapiens* genome encodes isoforms 1 and 2 (HsADA1 and HsADA2, respectfully), which differ in specific expression patterns, three-dimensional structure, and catalytic activity [2, 3]. While both enzymes convert adenosine to inosine and 2-deoxyadenosine to 2-deoxyinosine, the monomeric HsADA1 is largely present intracellularly with small amounts found extracellularly bound to CD26, while the homodimeric HsADA2 is secreted [4]. Additionally, the catalytic activity of HsADA1 is far greater than that of HsADA2 [5].

Certain mutations to HsADA1 that reduce its catalytic activity result in toxic accumulation of its substrates in lymphocytes and in varying degrees of severe combined immunodeficiency (ADA-SCID) [6, 7]. The relative activities of twenty-nine ADA-SCID-associated HsADA1 mutations have been estimated using an *E. coli* lysate-based assay which confirmed their steeply reduced catalytic activity [8]. One HsADA1 variant, in which an aspartic acid at residue 8 is mutated to an asparagine (Asp8Asn, or D8N), is less active than wildtype HsADA1, with a lower V_{max} that results in reduced HsADA1 activity in patient red blood cells and plasma, but is not associated with ADA-SCID [9–11]. The D8N variant has been correlated with elevated sleep pressure and decreased wakeful vigilance, assumedly through enhanced activation of the adenosinergic pathway via excess adenosine, though it is important to note though that sleep is a complex physiological function regulated by several other molecules. The D8N variant is also correlated with a lesser likelihood of hypertension [12], coronary artery disease [13, 14], schizophrenia [15], and shorter life expectancy [16, 17]. Interestingly, other mammalian ADA homologs such as *Bos taurus* (BtADA1) and *Mus musculus* (MmADA) enzymes, naturally have an asparagine at this site.

In theory, the monomeric and non-glycosylated HsADA1 is a prime candidate for bacterial expression. However, prior efforts to produce and purify HsADA1 from *E. coli* have resulted in yields less than 1 milligram per liter of culture at low purity, likely because the complex folding of higher-order mammalian proteins can be challenging for bacterial hosts [18–20]. Due to challenges associated with HsADA1 production, studies performed with BtADA1 or MmADA homologs have primarily driven understanding of ADA structure and function, as well as ADA1 inhibitor development and development of an enzyme replacement therapy for ADA-SCID. For instance, co-crystallization of an ADA1-CD26 complex was performed with BtADA1 [21]. 2-deoxyconformycin, an HsADA1 inhibitor that is a first-line treatment

Author Manuscript Author Manuscript Author Manuscript Author Manuscript

for Hairy Cell Leukemia, has been crystallized in complex with murine ADA [22, 23], and the first effective, rationally designed ADA1 inhibitor, EHNA, was synthesized to bind the BtADA1 active site [24]. Finally, polyethylene glycol-conjugated BtADA1 (PEG-BtADA1) is an approved enzyme replacement therapy for ADA-SCID [6, 7].

However, the properties of the human protein are unlikely to perfectly mirror those of its homologs, as BtADA1 and MmADA share ~88% and ~83% identity with HsADA1, respectively. In this vein, we recently demonstrated that the catalytic gate of the *holo* bovine ADA1 is in an "open" conformation while that of *holo* HsADA1 is in a "closed" conformation [2]. In addition, murine ADA does not bind CD26, while HsADA1's interaction with CD26 may impact immune function [25, 26]. The differences in amino acid sequence should also impact each enzyme's immunogenicity when used a therapeutic context. For instance, ADA-SCID patients can generate antibodies specific for BtADA1 that do not cross react with HsADA1 [27–29].

There are several methods that can be employed to improve expression and purification of human proteins in *E. coli*, including utilizing different *E. coli* expression strains or promoters, fusing human proteins to solubility tags, chilling cultures prior to induction or inducing at low temperatures, co-expressing chaperones, and the addition of chemical additives during the induction process [30–35]. In addition to expression considerations, modifying affinity tag design can enhance protein recovery and purity. Nickel ion (Ni^{2+}) immobilized metal affinity chromatography (IMAC) is routinely utilized to isolate recombinantly expressed histidine-tagged (his-tagged) proteins, often using a hexahistidine (His_6) tag placed at either the N- or C-terminus, which may also enhance expression or solubility [36, 37]. The length of a his-tag, i.e. the number of his residues that comprise it, can also impact the ability of the protein of interest to bind the nickel column [38].

Herein, we first validate a lysate-based assay to predict HsADA1 production in *E. coli*, and then use it to develop a reliable HsADA1 production protocol by improving several aspects of both the genetic construct and expression parameters. We then use our protocol to produce both wildtype HsADA1 and the D8N variant, and then compare their activities in a simulated physiological environment. We show that both enzymes have surprisingly enhanced activity in serum, likely due to an interaction with albumin that has yet to be characterized, and that the D8N variant may partially compensate for its reduced catalytic activity with improved stability in serum.

MATERIALS AND METHODS

Molecular cloning procedures and techniques

HsADA1 (UniProt P00813) and HsADA1 D8N gene fragments codon optimized for *E. coli* expression were purchased as oligonucleotide fragments from Twist Biosciences. Fragments were amplified with DNA oligomer primers (Eurofins Genomics) and the KOD Hotstart polymerase (EMD Millipore) as per the manufacturer's instructions. Primers for amplification (Supplementary Table 1) were designed to add overlapping regions to adjacent fragments for assembly as described by *Gibson* [39]. Plasmids were linearized with restriction enzymes purchased from New England Biolabs (pET-28 a (+) with NcoI and SalI,

Author Manuscript Author Manuscript Author Manuscript Author Manuscript

pMAL-C5X with MfeI and NcoI, pET28-MBP-TEV with BamHI and XhoI, and pGEX-4T2 with EcoRI and SalI) for 1 hour at 37°C. Amplified and linearized fragments with sufficient overlap were assembled via the method originally described by *Gibson* [39]. In brief, 0.02–0.1 pmol of each fragment was added to a mastermix containing T5 exonuclease (New England Biolabs), Taq DNA Ligase (Enzymatics), and Phusion polymerase (New England Biolabs) and incubated at 50°C for 1 hour. Prior to electroporation into *E. coli*, Gibson reactions were dialyzed against ultrapure water using 0.025μm filter membranes (Millipore) for 20 minutes. Following transformation into *E. coli* and selection, plasmids were extracted from 6mL cultures with the Qiagen Miniprep Kit and sent to Eurofins Genomics, Genewiz from Azenta Life Sciences, or Georgia Tech Molecular Evolution Core for sequencing.

Construction of HsADA1 tagged constructs and the D8N variant

The first HsADA1 sequence codon optimized for *E. coli* (HsADA1_1.0) was purchased with a N-terminus His_6 tag (N-His_6) and amplified for insertion into pET-28 a (+) and pMAL-C5X with primers 1 & 2 and 3 & 4, respectively. Two amplifications were employed to switch the His_6 tag flanking HsADA1_1.0 from the N- to the C-terminus for placement into pET-28 a (+): first with primers 5 & 6 followed by 5 & 7 to generate the final HsADA1_1.0 C-His_6 gene product with overlap for the pET-28 a (+) on both the 5' and 3' ends of the gene. Sequences for HsADA1_1.0 C-His_6 fused to an additional His_6, octahistidine, or decahistidine tag (resulting in his-tags denoted as C-His_6-His_6, C-His_6-His_8, or C-His_6-His10, respectively) with pET-28 a (+) overlap were generated by amplification of the HsADA1_1.0 C-His_6 gene with primers 16 & 17, 16 & 18, and 16 & 19, respectively. Full amino acid sequences for the his-tags used in this study are listed in Supplementary Table 2. In contrast to HsADA1_1.0, the second HsADA1 codon optimized sequence (HsADA1_2.0) was purchased with a C-His_6 tag and amplified for placement into pET-28 a (+) and pMAL-C5X with primers 8 & 9 and 10 & 11, respectively.

The D8N mutation was incorporated into HsADA1_1.0 C-His_6-His_{10} through generation of two amplified fragments with overlap at the D8N codon switch (primers 20 & 21, and 26 & 27), and then the rest of the plasmid was amplified in two more fragments (primers 22 & 23, and 24 & 25) and reconstructed with Gibson Assembly. N-terminus maltose-binding protein (MBP) and glutathione S-transferase (GST) fusions to HsADA1 C-His_6 were generated by amplification of HsADA1 C-His_6 with primers 12 & 13 and 14 & 15, respectively, and insertion into the linearized pET28-MBP-TEV and pGEX-4T2 plasmids via Gibson Assembly.

E. coli strains and culturing techniques

Plasmids were amplified in strains 5-alpha, 10-beta, or Stable, and protein expression was performed in T7 Express or C43(DE3), of which all except C43(DE3) were purchased from New England Biolabs. Plasmid selection following transformation occurred on LB-agar plates (2.5%$^{w}/_{v}$ LB (Teknova) and 2%$^{w}/_{v}$ agar (Fisher Bioreagents)) and single colonies were transferred to six milliliters (6 mL) of LB for overnight incubation at 37°C and 250 RPM. 50 μg/mL kanamycin sulfate (Sigma Aldrich) was added to solid and liquid media to select for pET-28 a (+) and pET28-MBP-TEV plasmids, and 100 μg/mL ampicillin sulfate (Sigma Aldrich) was used to select for pGEX-4T2 plasmids.

Author Manuscript Author Manuscript Author Manuscript Author Manuscript

Strains for protein expression were first selected for on LB-Agar plates and in LB preculture. Precultures were used to inoculate terrific broth, or TB (Invitrogen), with appropriate antibiotic at a dilution of 1:100. Cultures were grown at 37°C with agitation until an OD600 between 0.9 and 1.0. Cultures to be induced at temperatures below 37°C were placed on an ice-water slurry for 30 minutes prior to induction. At induction, isopropyl β-D-1-thiogalactopyranoside (IPTG, Fisher Bioreagents) was added to TB cultures to a final concentration of 0.5 mM, and if applicable, ethanol was added as well. Cultures were then agitated up to 73 hours prior to pelleting in a centrifuge chilled to 4°C at 3,400 × g, followed by storage at −80°C.

Absorbance measurements

Adenosine (TCI or Sigma Aldrich) or inosine (TCI) were added to ultrapure water to a final stock concentration of 5mM and dissolved by turning end-over-end for 30 minutes. Diluted standards were generated via dilution of stock into PBS pH 7.4. All absorbance measurements were performed using UV-compatible flat-bottom 96-well microplates (Corning 96-well UV-transparent microplates or Greiner Bio-One 96 well UV-Star microplates) and the BioTek Synergy HT Microplate Reader. All measurements occurred at 25°C with absorbance read from the bottom of wells containing 200 μL solution. Kinetic measurements were performed with minimal time between readings as determined by the Synergy software.

96 Deep-Well Plate Culture Condition Screening

Individual T7 Express colonies containing expression plasmids in 200 uL of LB media were pre-cultured overnight in a 96-well U-bottom microplates (Eppendorf) at 300 RPM and 37°C. One microliter (1 μL) of overnight culture was used to inoculate a well containing 1000 μL of TB media in a second deep-well plate (expression plate). The expression plate was incubated at 300 RPM and 37°C for five hours. Following addition of IPTG and a single bolus of ethanol, if applicable, the expression plate was returned to incubation at 300 RPM and the desired induction temperature. At noted time points, 50 μL of culture was transferred into 96-well U-bottom microplate (sampling plate), pelleted at 4°C and 3400 × g for 10 minutes. Supernatant was discarded, and plates were moved to a −80°C freezer for storage.

To obtain *E. coli* lysates for analysis, the sampling plates were thawed on an ice-water slurry and cell pellets were resuspended in 40 μL complete BPER lysis buffer (Thermo Scientific). The sampling plates were set to rock gently at room temperature for 15 minutes followed by centrifugation at 4°C and 3400 × g for 30 minutes. 50 μL of supernatant was removed from each well and transferred to a fresh 96-well U-bottom microplate. Two microliters (2 μL) of each supernatant was added to UV-compatible flat-bottom 96-well microplates and diluted with 38 μL phosphate buffered saline (PBS) pH 7.4. PBS pH 7.4 was formulated to final concentrations of 137 mM sodium chloride, 2.7 mM potassium chloride, 10 mM sodium phosphate dibasic, and 1.8 mM potassium phosphate monobasic in ultrapure water (all chemicals purchased from Sigma Aldrich) [40]. 160 μL of 312.5 μM adenosine in PBS pH 7.4 was added to each well containing the diluted lysate solution for a final adenosine concentration of 250 μM and measurements of 260 nm absorbance were recorded for five minutes.

Author Manuscript Author Manuscript Author Manuscript Author Manuscript

Quantification of HsADA1 activity in *E. coli* lysate samples

We compared HsADA1 activity between *E. coli* lysates by employing a similar method to that described in *Gracia et al.* [41], which correlates absorbance signal loss with ADA in the *E. coli* lysates as performed by *Kalckar* [42], but modified for a microplate format as described by *Lu et al.* [43]. These methods are based in Beer's law and the disparate spectral profiles of adenosine and inosine absorbance [44, 45]. As described by *Lu et al.*, we first confirmed that the adenosine and inosine concentrations (C) used in the study correlated linearly with the measured absorbances (A) depicted in Supplementary Figure 1 as per the Beer-Lambert law (Equation 1).

$$A = \varepsilon \times L \times C \quad \text{(Equation 1)}$$

Then we used the change in absorbance with respect to time ($\Delta A260/s$) as a linear correlate for HsADA1 activity to compare expression conditions [43].

Expression and purification of HsADA1 protein for further analyses

Overnight starter culture was used to inoculate one liter (1 L) of TB at a 1:100 dilution, which was expanded to an OD600 of ~1.0, chilled, induced with IPTG and supplemented with 3%$^{v}/_{v}$ ethanol as a single bolus. Following a 48-hour induction at 15°C, the expression culture was pelleted in a 1 L Nalgene bottle, resuspended in PBS pH 7.4 and pelleted once more prior to storage at −80°C.

To lyse the cells, the pellet was resuspended in 100 mL of bind buffer (20mM sodium phosphate pH 7.4, 300 mM sodium chloride, 20 mM imidazole, all purchased from Sigma Aldrich). Once resuspended, 1 mg/mL lysozyme (Thermo Scientific), 1 mM PMSF (Fisher Bioreagents), and 10 U/mL Universal Nuclease (Pierce) were added. In a 100 mL graduated cylinder surrounded by an ice-water slurry, the resuspended pellet was sonicated with a Qsonica ½" tip for 40 mins (5 seconds on, 5 seconds off) at 30% amplitude. The resulting lysate was centrifugated at 20,000 × g and 4°C for 1 hour.

Using a Cytiva AKTA Go, the cell lysate was fed over a Cytiva Histrap HP one milliliter (1mL) nickel column equilibrated with bind buffer at a rate of 1 mL/min at 4°C. The column was washed with 20 column volumes (CV) of bind buffer followed by a gradient elution from 0–100% elution buffer (20 mM sodium phosphate pH 7.4, 300 mM sodium chloride, 500 mM imidazole) over the course of 20 CV followed by an additional 5 CV with 100% elution buffer during which fractions were collected in 1.5 CV increments.

Four microliter (4 μL) samples from the IMAC purification sequence, i.e., the clarified lysate, clarified lysate after flowing through the column, collected bind buffer used to wash the column following lysate load, and the gradient elution fractions were prepared for SDS-PAGE analysis using 2X Laemlli sample buffer (Bio Rad) and TCEP Bind-Breaker (Invitrogen) and denatured at 95°C for five minutes. TGX Stain-Free agarose gels for PAGE electrophoresis (Bio-Rad) were prepared and run under denaturing conditions (25 mM tris, 192 mM glycine, and 0.1% sodium dodecyl sulfate, all chemicals purchased from Sigma Aldrich). Fractions containing HsADA1 were pooled and subjected to size exclusion

Author Manuscript Author Manuscript Author Manuscript Author Manuscript

chromatography (SEC) via the AKTA Go system at 4°C with a HiLoad Sephacryl S-200 HR column equilibrated with running buffer (50 mM sodium phosphate pH 7.4, 150 mM sodium chloride). Pure fractions were pooled and concentrated using a 10 kDa Amicon centrifugal concentrator (Millipore) and the final protein concentration was determined with the Pierce BCA Protein Assay Kit (Thermo Scientific). Two microgram (2 μg) samples of the final product following SEC and concentration were prepared as previously described for the IMAC sequences samples and analyzed for purity following SDS-PAGE with the Bio-Rad Image Lab software.

Differential Scanning Fluorimetry

Differential scanning fluorimetry (DSF) was employed to determine the melting temperatures (T_m) of HsADA1 C-His_6-His_{10} and HsADA1 D8N C-His_6-His_{10}. Protein samples at a concentration of 1 mg/mL in PBS pH 7.4 were loaded into PROMETHEUS NT.48 glass capillaries and loaded into the NanoTemper PROMETHEUS NT.48 NanoDSF. With the temperature raised from 20°C to 90°C at a rate of 0.1°C/min, the Nanotemper PR.ThermoControl version 2.1.5 software determined the inflection point of the 330 nm to 350 nm absorbance ratio curve as the melting temperature. Six sample replicates were tested for each T_m determination.

Determination of Michaelis-Menten kinetic parameters

Wells in a UV-compatible 96-well plate containing adenosine dissolved in PBS pH 7.4 at initial concentrations from 0 μM to 250 μM and known HsADA1 (or D8N variant) concentrations were monitored for A260 signal loss (ΔA260/time) as with the *E. coli* lysate samples described earlier. We then fit the calculated absorbance change rates and associated initial adenosine substrate concentrations to the Michaelis-Menten model (Equation 2) as described in *Lu et al.* [43] to determine the enzyme substrate affinity (K_M) and maximum reaction rate (V_{max}) in the units of molarity and $\Delta A260/time$, respectively.

$$Rate = \frac{V_{max}[Substrate]}{K_M + [Substrate]} \quad \text{(Equation 2)}$$

We next determined the term composed of the extinction coefficient (ε) and pathlength (L) for both adenosine and inosine and subtracted the lesser inosine value from the adenosine value as described by both *Gracia et al.* and *Lu et al.* for a $L\Delta\varepsilon$ value of 4646 L/mol (Supplementary Figure 1). The Beer-Lambert law modified for change is depicted below (Equation 3).

$$\Delta A = \Delta\varepsilon \times L \times \Delta C \quad \text{(Equation 3)}$$

Once we determined the 260 nm absorbance rate of change with respect to time (ΔA260/time or ΔA) we divided that quantity by $L\Delta\varepsilon$ to obtain the change in adenosine with respect to time ($\Delta[adenosine]/time$ or ΔC) due to addition of the lysate sample (Equation 4).

Author Manuscript Author Manuscript Author Manuscript Author Manuscript

$$\Delta[C] = \frac{\Delta A}{L \times \Delta \varepsilon} \quad \text{(Equation 4)}$$

Then, we converted the V_{max} unit to $^{Molarity}/_{time}$ by rearranging the Beer-Lambert law modified for change with respect to time to solve for concentration (Equation 3) also as described by *Lu et al.* [43]. To calculate specific activity in the unit of $^{\mu mol\ adenosine}/_{min\ -\ mg\ enzyme}$, we first converted the enzyme concentration from molarity to $^{mass}/_{volume}$ (in units of $^{mg\ enzyme}/_{L}$ (Equation 5), then divided the value from the V_{max} (Equation 6).

$$\left(\frac{nmol\ enzyme}{L}\right) \times \left(\frac{mol}{10^9\ nmol}\right) \times \left(\frac{g\ enzyme}{mol\ enzyme}\right) \times \left(\frac{10^3 mg}{g}\right) = \left(\frac{mg\ enzyme}{L}\right) \quad \text{(Equation 5)}$$

$$Specific\ activity = \frac{V_{max}\left(\frac{\mu mol\ adenosine}{min\ -\ L}\right)}{[enzyme]\left(\frac{mg\ enzyme}{L}\right)} = \left(\frac{\mu mol\ adenosine}{min\ -\ mg\ enzyme}\right) \quad \text{(Equation 6)}$$

To calculate the turnover number (k_{cAT}), we divided the V_{max} quantity by the total enzyme concentration ($[E]_{total}$) (Equation 7).

$$k_{CAT} = \frac{V_{max}}{[E]_{total}} \quad \text{(Equation 7)}$$

Lastly, we calculated catalytic efficiency as the ratio between turnover number k_{CAT} and the substrate affinity (K_M) (Equation 8).

$$Catalytic\ Efficiency = \frac{k_{CAT}}{K_M} \quad \text{(Equation 8)}$$

Determination of catalytic activity from HsADA1 samples in the presence of bovine serum albumin or human serum

HsADA1 C-His_6-His_{10} and HsADA1 D8N C-His_6-His_{10} were added at a final concentration of one micromolar (1μM) to 45mg/mL bovine serum albumin (BSA, Sigma Aldrich) in PBS pH 7.4, to PBS pH 7.4, or to pooled human serum (MP Biomedicals). Activity was determined in in a UV-compatible microplate (Corning or Greiner BioOne) well containing 200 μL of 250 μM adenosine and enzyme mixture diluted 1:50 in PBS pH 7.4 by monitoring absorbance at 260 nm. Baseline activity for these solutions was determined by measuring the activity of the enzyme in PBS pH 7.4. For time-course experiments at 37°C, sample replicates were stored in Protein LoBind tubes (Eppendorf) with the caps sealed with parafilm (VWR). The tubes were placed in a cabinet incubator set to 37°C and sampled after 48 hours.

Author Manuscript Author Manuscript Author Manuscript Author Manuscript

Statistical analysis

All statistical analyses herein (t-tests and ANOVAs) were performed with GraphPad Prism 9. *Post-hoc* multiple comparisons were performed following ANOVA with correction to *p-values* as per the Holm-Šídák method, where significance between pairs is denoted as **p<0.05, **p<0.01, ***p<0.001, ****p<0.0001.*

RESULTS

Screening and improving HsADA1 expression conditions in *E. coli*

As modulating transcriptional level can be particularly useful towards improving human recombinant protein production in *E. coli*, we first performed testing of the impact of using the C43(DE3) expression strain, which has reduced T7 polymerase activity, for HsADA1 production, as well as the impact of using the hybrid tac promoter instead of the viral T7 promoter [46, 47]. Preliminary IMAC gravity purification demonstrated a clear benefit to controlling HsADA1_1 with the T7 promoter (pET-28 a (+) plasmid), over the tac promoter (pMAL-C5X plasmid) and no detectable difference between using the C43(DE3) expression strain compared to the T7 Express strain (Supplementary Figure 2).

We next calculated the level of ADA activity in *E. coli* lysates encoding different codon optimized versions of the HsADA1 gene, dubbed HsADA1_1.0 and HsADA1_2.0, at two induction temperatures (15°C and 37°C) (Figure 1A–B). We compared the HsADA1 activity in the *E. coli* lysates by employing a similar method to that described in *Gracia et al.* [41], which correlates absorbance signal loss with ADA activity in *E. coli* lysates, but modified for a microplate format [42, 43]. These methods take advantage of the different spectral profiles of adenosine and inosine absorbance [44, 45]. Therefore, we used change in absorbance with respect to time ($\triangle A260/s$) as a correlate for HsADA1 activity to compare expression conditions [43]. Maximum HsADA1 activity was detected in the lysate samples at the final timepoint tested for all conditions (21-hours induction), with lysates from *E. coli* encoding HsADA1_1.0 induced at 15°C exhibiting the highest HsADA1 activity levels. Being that each codon optimized cassette encodes an identical HsADA1 enzyme and is controlled by the same promoter, differences in lysate activity result from differing levels of properly folded HsADA1 [48]. We again tested the impact of expression strain (C43 versus T7 express) for both codon-optimized sequences, but again saw no detectable difference in HsADA1 content within the lysates of the respective strains as per SDS-PAGE (Supplementary Figure 2). Thus, we utilized the HsADA_1.0 codon optimized gene sequence and the T7 expression strain for future experiments.

Next, we considered if His_6 tag placement could improve HsADA1 expression, as gauged via activity in lysate, again assaying multiple induction temperatures [38, 49]. As the 15°C induction resulted in far higher lysate activity than at 37°C, we compared 15°C to an intermediate temperature, 25°C. We were also interested in determining if lengthening the induction period could enhance enzyme production, as implied by our initial studies (Figure 1A). Therefore, we evaluated the lysate activity of HsADA1 with either a N-His_6 or C-His_6 tag at 15°C and 25°C over a 69-hour induction period (Figure 1C–D).

Author Manuscript Author Manuscript Author Manuscript Author Manuscript

By comparing the maximum HsADA1 lysate activity for each condition across the induction period (testing at 4, 20, 48, and 69 hours), we discerned that 69 hours' induction time at 15°C for the HsADA1 C-His_6 construct yielded the highest lysate activity, although this was not significant compared to the same construct's production at 48 hours nor the HsADA1 N-His6 construct's activity after 48 hours at 15°C (Figure 1C). In general, His_6 tag placement had little impact on HsADA1 expression, while 15°C induction and longer induction times (at least 48 hours) were a strict requirement for enhanced HsADA1 production (Figure 1D). As we had seen that the lowest tested induction temperature (15°C) consistently improved HsADA1 expression, we also explored further temperature reduction to using the engineered ArcticExpress (DE3) strain, but we saw poor viability and did not detect lysate HsADA1 activity (data not shown). Therefore, we performed further lysate-based experiments using the HsADA1 C-His_6 with the 15°C induction temperature and induction times of greater than or equal to 48 hours.

In the presence of ethanol, *E. coli* upregulate expression of heat-shock proteins that can act as molecular chaperones to enhance recombinant protein expression [33, 50, 51]. Therefore, we next tested if the addition of ethanol could increase HsADA1 production, initially comparing 0%$^{v}/_{v}$, 3%$^{v}/_{v}$, and 5%$^{v}/_{v}$ ethanol supplementation during induction (Figure 2). Addition of 3%$^{v}/_{v}$ ethanol consistently resulted in enhanced lysate HsADA1 activity relative to 0%v/v ethanol addition across the length of induction, while 5%$^{v}/_{v}$ ethanol addition provided no benefit until after 68 hours (Figure 2). The 3%$^{v}/_{v}$ ethanol supplementation reached maximal enzyme production within 45 hours. Interestingly, when we again compared the impact of His_6 tag placement in the context of ethanol addition, we saw that the C-His_6 construct afforded enhanced HsADA1 expression relative to the N-His_6 construct (Supplementary Figure 3). We also tested if reducing ethanol levels to 1%$^{v}/_{v}$ or 2%$^{v}/_{v}$ could enhance HsADA1 expression, but saw no benefit compared to 3%$^{v}/_{v}$ ethanol (data not shown).

Fusion with an extremely soluble partner protein such a glutathione S-transferase (GST) or maltose-binding protein (MBP), whose proper folding can rescue the target protein from misfolding and aggregating in inclusion bodies, can enhance the solubility of a recombinant protein in the *E. coli* cytoplasm [52–54]. Therefore, we tested if fusion of HsADA1 C-His_6 with solubility tags would improve its expression. However, neither MBP nor GST enhanced HsADA1 expression (Supplementary Figure 4). While expression of the MBP-HsADA1 C-His_6 lysate activity was comparable to lysate activity in the absence of the MBP tag, lysate activity with the GST construct was severely diminished, however, it is important to note that the MBP construct was under the control of the T7 promoter in the pET-28-MBP-TEV plasmid and the GST was under the control of the tac promoter in the pGEX-4T2 plasmid. Therefore, the ineffectiveness of the GST construct towards enhancing HsADA1 expression in lysate may be due to incompatibility with the tac promoter.

A double-histidine tag significantly improves the purity of recombinantly expressed HsADA1

His_6 tag fusions can allow for more than 90% purity of recombinant proteins following Ni^{2+} IMAC [55, 56]. However, when a protein is expressed at lower levels, purity is

Author Manuscript Author Manuscript Author Manuscript Author Manuscript

often reduced. The addition of more histidine residues to the His_6 tag has been shown to strengthen binding to the Ni^{2+} column, allowing for the use of stronger wash conditions to remove impurities [57]. In the same vein, adding two His_6 tags in tandem, i.e. a double-his-tag (e.g., His_6-His_6), also results in greater binding affinity to the nickel column, which can improve protein purity [58].

Therefore, we sought to determine if utilizing double and/or lengthened his-tags could improve the purity of HsADA1 following a gradient elution. More specifically, we compared elution fractions of HsADA1 C-His_6 with the double-his-tagged combinations C-His_6-His_6, C-His_6-His_8, and C-His_6-His_{10} on SDS-page. A schematic of the elution sequence is available in Supplementary Figure 5, and using gradient elution of IMAC bound protein from 20 mM to 500 mM imidazole allows for proteins with higher affinity for the column to elute in later fractions than proteins with lesser affinity. We saw that HsADA1 C-His_6 eluted mostly in fractions 7–9 (272 mM-344 mM imidazole), but as hoped, double-his-tagged combinations C-His_6-His_6, C-His_6-His_8, and C-His_6-His_{10} eluted later, primarily between fractions 9–12 (344 mM-458 mM imidazole), 10–13 (380 mM-488 mM imidazole), and 11–14 (416 mM-500 mM imidazole), respectively, (Figure 3, Supplementary Figure 6). The final size exclusion product for each of these purifications are in the “S” lanes and are analyzed for purity in Figure 4.

Promisingly, across three purification replicates, the size exclusion product of HsADA1 C-His_6-His_{10} was 94.93 ± 0.603 % pure versus the average 79.17 ± 3.10 % purity of the HsADA1 C-His_6 construct, likely because the C-His_6-His_{10} construct experienced a more stringent wash while on-column before eluting (Figure 4). Under the optimized expression conditions determined with the lysate-based assays, we recovered 5 ± 0.5 mg (n=3) of pure HsADA1 C-His_6-His_{10} per liter of *E. coli* culture following affinity and size exclusion chromatography.

Characterization of the HsADA1 D8N variant reveals reduced catalytic efficiency but enhanced retention of activity at physiological conditions

Using our optimized HsADA1 expression conditions and the double-C-His_6-His_{10} affinity tag, we purified the HsADA1 D8N variant (Figure 5, Supplementary Figure 7).

HsADA1 D8N is less active than its wildtype counterpart with Michaelis-Menten parameters of $K_M = 21.83 \pm 2.19$ μM, $V_{max} = 1.33*10^{-4} \pm 3.60*10^{-6}$ $\Delta A260/s$ (or 28.65 ± 0.77 nM adenosine/s), specific activity $= 158.79 \pm 4.29$ $\mu mol\ adenosine/min - mg\ D8N$, and $k_{CAT} = 114.59 \pm 3.10\ s^{-1}$ ($[E]_{total} = 0.25$nM) for a catalytic activity of $k_{CAT}/K_M = 5.25 \times 10^6 M^{-1}\ s^{-1}$ (Figure 5A) versus the wildtype enzyme’s $k_{CAT}/K_M = 7.15 \times 10^6 M^{-1}\ s^{-1}$ [2]. This is in close agreement with results reported by *Riksen et al.* [11], that the D8N variant is ~27% less active than wildtype HsADA1. HsADA1 D8N also has a slightly lower melting temperature than the wildtype enzyme, 55.5 ± 0.2 °C versus 60.1 ± 0.3 °C, respectively (Figure 5B).

Interestingly, both wildtype HsADA1 and the D8N mutant lose their activity when incubated in human serum at 37°C, i.e., physiologically mimicking conditions (Figure 5C), however,

Author Manuscript Author Manuscript Author Manuscript Author Manuscript

D8N retained its activity to a greater extent than the wildtype enzyme. Specifically, D8N retained 74.3 ± 1.5% of its original activity while wildtype retained 62.4 ± 1.0% after a 48-hour incubation in serum at 37°C.

Wildtype HsADA1 and the D8N variant exhibit enhanced activity in the presence of serum, potentially due to albumin

In evaluating the activity retention of HsADA1 and HsADA1 D8N in human serum, we noticed that activities of each enzyme, as gauged by catalytic rate at a saturating adenosine concentration, increased by 2.10 ± 0.07-fold (Figure 6A) and 1.82 ± 0.08-fold (Figure 6B), respectively, in serum compared to in PBS pH 7.4. As albumin is by far the most prevalent protein in serum, with typical levels in humans around 45 mg/mL, we were interested to see if it could be driving this effect [60, 61]. Both wildtype HsADA1 and HsADA1 D8N activity increased when in 45 mg/mL BSA (PBS pH 7.4) compared to normal PBS, i.e., the activity of wildtype increased by 1.55 ± 0.06-fold (Figure 6A) and that of D8N increased by 1.36 ± 0.06-fold (Figure 6B), suggesting that an interaction between albumin and HsADA1 is partially responsible for this phenomenon. The activity of wildtype HsADA1 increased more in the presence of BSA and serum than that of the D8N variant (Figure 6C).

DISCUSSION

Our initial attempts to produce HsADA1 in *E. coli* yielded less than 1mg/L of culture of low-purity protein, as had been seen in a prior attempt to produce this enzyme [20]. To optimize HsADA1 expression with respect to multiple expression parameters, we used a bacterial lysate-based assay to screen several conditions for HsADA1 production in the *E.coli* strain T7 Express, using the adenosine-deaminating activity within lysate as a proxy for soluble HsADA1 levels. We used our lysate-based activity assay to test two codon optimized forms of the HsADA1 gene (HsADA1_1.0 and HsADA1_2.0), three induction temperatures (15°C, 25°C, and 37°C), His_6 tag fusion to both the N- and C-terminus, the N-terminus fusion of two solubility tags (MBP and GST) to the HsADA1 C-His_6 construct, ethanol supplementation from 0%$^{v}/_{v}$ to 5%$^{v}/_{v}$, and induction time from 0 to 73 hours in a multiplexed manner (Figures 1 & 2). We determined that the HsADA1 His_6 construct induced at 15°C with 3%$^{v}/_{v}$ ethanol supplementation for two or more days resulted in the highest expression of recombinant enzyme. Both low induction temperature and long induction times helped increased HsADA1 production, while altering promoter choice or expression strain had negligible or negative impact (Supplementary Figure 2). As promoter choice and expression strain (C43 versus T7 express) would be expected to primarily impact transcriptional rates, it is likely that modulating aspects of HsADA1 translation were key to improving its production in *E. coli*. Still, lowering induction temperature does reduce both transcriptional and translational rates, suggesting that there may be an optimal tradeoff that the lysate-based assay was helpful towards finding.

We initially found that the final product of the HsADA1 C-His_6 purification was low purity even after SEC, assumedly due to routine contamination with endogenous *E. coli* proteins that occurs for proteins that are not expressed highly (Figure 4) [57, 62, 63]. As low protein purity can preclude accurate downstream characterization or structural studies, we attempted

Author Manuscript Author Manuscript Author Manuscript Author Manuscript

to reduce the prevalence of these contaminants. High histidine content in endogenous *E. coli* proteins can decrease the purity of Ni^{2+} IMAC purifications, and certain *E. coli* proteins that lack metal-binding domains, such as GroEL/Hsp60, also interact and co-elute with recombinant proteins [62–65]. With the goal of being able to perform more stringent wash steps, we attempted to improve the purity of HsADA1 by increasing its column affinity through the addition of histidine residues to its purification tag via a double-his-tag construct [58]. As hoped, addition of a second His_6 tag in tandem to the first (C-His_6-His_6) resulted in elution of HsADA1 product at a higher imidazole concentration than the C-His_6 construct, at 272 mM versus 344 mM, respectively (Figure 3). Additions of His_8 and His_{10} tags to the first C-His_6 tag (C-His_6-His_8 and C-His_6-His_{10}, respectively) allowed for the protein to remain on column to even higher imidazole concentrations, and the C-His_6-His_{10} HsADA1 eluted last in our gradient elution scheme as it would be expected to if it had the highest affinity for the IMAC column. As HsADA1 C-His_6-His_{10} product was significantly purer than HsADA1 C-His_6 (Figure 4), increased HsADA1 column affinity and subsequent pre-elution of contaminants appeared to successfully increase its purity.

To demonstrate the utility of our improved HsADA1 expression and purification process, we produced the HsADA1 D8N variant, which has not yet purified to homogeneity and characterized [66]. We were able to successful produce up to 5 mg/L of >90% purity HsADA1 D8N protein on the first attempt using our new system, which allowed for facile determination of its kinetic parameters, melting temperature, and behavior in human serum at body temperature. We confirmed that the D8N variant is ~30% less active than wildtype HsADA1 [11] and showed that it better retains activity under physiologically mimicking conditions, i.e., incubation in human serum at 37°C (~74% versus ~62% after 48 hours) (Figure 5). Therefore, the D8N variant's ability to retain activity in serum may help offset its reduced activity.

As an additional benefit enabled by our platform, while we were studying the HsADA1 wildtype and D8N activity in human serum, we noticed that HsADA1 is ~2-fold more active in serum than in PBS pH 7.4 (Figure 6). Serum contains numerous macromolecules, metabolites, and other components, but albumin accounts for most of serum's protein content with typical concentrations of 35 mg/mL to 45mg/mL [60, 61, 67]. Therefore, we went on to show that the addition of only bovine serum albumin in PBS pH 7.4 could similarly enhance HsADA1 activity, though not to the full extent as in human serum (Figure 6B).

CONCLUSIONS

We have developed a robust framework for optimizing the expression and recovery of HsADA1 from an *E. coli* host and demonstrated its utility by purify, characterizing, and comparing wildtype enzyme and its D8N variant. With purified proteins, we also demonstrate a previously unreported interaction of human serum that increases the activity of HsADA1 and identify albumin as a contributor to this effect. Our purification framework should allow for specific characterization of other HsADA1 variants of clinical relevance, as well as general studies into HsADA1 function. For instance, our higher-titer, high purity HsADA1 production method could enable future structural studies of HsADA1, such as

Author Manuscript Author Manuscript Author Manuscript Author Manuscript

of co-crystal structures with its receptor CD26 or in complex with enzyme inhibitors, as prior structural characterizations in this vein have been produced using the bovine and mouse ADA1 homologs [2, 21, 22, 68–74]. Efficient production of HsADA1 could also allow therapeutic development of the enzyme itself. In this vein, bovine ADA1 is an FDA-approved ADA-SCID therapy, and both bovine ADA1 and the less active human ADA1 isoform, HsADA2, have been shown efficacy in preclinical studies as cancer immunotherapeutics [75–79]. To be best of our knowledge, HsADA1 has not been tested for these applications, potentially due to prior difficulties in its production.

Supplementary Material

Refer to Web version on PubMed Central for supplementary material.

ACKNOWLEDGEMENTS

We thank Julie A. Champion (School of Chemical & Biomolecular Engineering at Georgia Tech) for the pET-28a and pGEX-4T2 plasmids, Vinny Agarwal (School of Chemistry and Biochemistry at Georgia Tech) for the pET28-MBP-TEV plasmid and Raquel Lieberman (School of Chemistry and Biochemistry at Georgia Tech) for the C43(DE3) *E. coli* strain and the pMAL-C5X plasmid.

FUNDING SOURCES:

MRJ is supported by a National Science Foundation Graduate Research Fellowship. JB receives funding from the Emory University Winship Cancer Center through its Career Enhancement Program (NIH Award Number P50CA217691), the Arnold and Mabel Beckman Foundation, a Georgia Institute of Technology Petit Institute of Bioengineering and Biosciences seed grant, and the NIH (Award Number 1DP2CA280622–01). The content is solely the responsibility of the authors and does not necessarily reflect the official views of the National Science Foundation, the National Institutes of Health, the Winship Cancer Center, or the Beckman Foundation.

Data Statement:

Raw data generated over the course of experiments is available upon reasonable request.

REFERENCES

1. Van der Weyden MB and Kelley WN, Human adenosine deaminase. Distribution and properties. J Biol Chem, 1976. 251(18): p. 5448–56. [PubMed: 9388]
2. Ma MT, et al. , Catalytically active holo Homo sapiens adenosine deaminase I adopts a closed conformation. Acta Crystallogr D Struct Biol, 2022. 78(Pt 1): p. 91–103. [PubMed: 34981765]
3. Zavialov AV and Engstrom A, Human ADA2 belongs to a new family of growth factors with adenosine deaminase activity. Biochem J, 2005. 391(Pt 1): p. 51–7. [PubMed: 15926889]
4. Zavialov AV, et al. , Human adenosine deaminase 2 induces differentiation of monocytes into macrophages and stimulates proliferation of T helper cells and macrophages. J Leukoc Biol, 2010. 88(2): p. 279–90. [PubMed: 20453107]
5. Luo W, et al. , ELISA based assays to measure adenosine deaminases concentration in serum and saliva for the diagnosis of ADA2 deficiency and cancer. Front Immunol, 2022. 13: p. 928438. [PubMed: 35967411]
6. Kwan A, et al. , Newborn screening for severe combined immunodeficiency in 11 screening programs in the United States. JAMA, 2014. 312(7): p. 729–38. [PubMed: 25138334]
7. Flinn AM and Gennery AR, Adenosine deaminase deficiency: a review. Orphanet J Rare Dis, 2018. 13(1): p. 65. [PubMed: 29690908]
8. Arredondo-Vega FX, et al. , Adenosine deaminase deficiency: genotype-phenotype correlations based on expressed activity of 29 mutant alleles. Am J Hum Genet, 1998. 63(4): p. 1049–59. [PubMed: 9758612]

Author Manuscript Author Manuscript Author Manuscript Author Manuscript

9. Battistuzzi G, et al. , Comparative activity of red cell adenosine deaminase allelic forms. Nature, 1974. 251(5477): p. 711–3. [PubMed: 4427666]
10. Fattahi A, et al. , The Role of G22 A Adenosine Deaminase 1 Gene Polymorphism and the Activities of ADA Isoenzymes in Fertile and Infertile Men. Urology, 2015. 86(4): p. 730–4. [PubMed: 26166670]
11. Riksen NP, et al. , The 22G>A polymorphism in the adenosine deaminase gene impairs catalytic function but does not affect reactive hyperaemia in humans in vivo. Pharmacogenet Genomics, 2008. 18(10): p. 843–6. [PubMed: 18794722]
12. Gloria-Bottini F, et al. , Smoking and hypertension: Effect of adenosine deaminase polymorphism. Clin Exp Hypertens, 2019. 41(6): p. 548–551. [PubMed: 30192643]
13. Saccucci P, et al. , Coronary artery disease. A study of three polymorphic sites of adenosine deaminase gene. Acta Cardiol, 2014. 69(1): p. 39–44. [PubMed: 24640520]
14. Safranow K, et al. , ADA*2 allele of the adenosine deaminase gene may protect against coronary artery disease. Cardiology, 2007. 108(4): p. 275–81. [PubMed: 17287605]
15. Dutra GP, et al. , Lower frequency of the low activity adenosine deaminase allelic variant (ADA1*2) in schizophrenic patients. Braz J Psychiatry, 2010. 32(3): p. 275–8. [PubMed: 20414589]
16. Napolioni V and Lucarini N, Gender-specific association of ADA genetic polymorphism with human longevity. Biogerontology, 2010. 11(4): p. 457–62. [PubMed: 20174870]
17. Napolioni V, et al. , Age- and gender-specific epistasis between ADA and TNF-α influences human life-expectancy. Cytokine, 2011. 56(2): p. 481–8. [PubMed: 21865054]
18. Mierendorf RC, et al. , Expression and Purification of Recombinant Proteins Using the pET System. Methods Mol Med, 1998. 13: p. 257–92. [PubMed: 21390849]
19. Dyson MR, et al. , Production of soluble mammalian proteins in Escherichia coli: identification of protein features that correlate with successful expression. BMC Biotechnol, 2004. 4: p. 32. [PubMed: 15598350]
20. Gracia E, et al. , Human adenosine deaminase as an allosteric modulator of human A(1) adenosine receptor: abolishment of negative cooperativity for [H](R)-pia binding to the caudate nucleus. J Neurochem, 2008. 107(1): p. 161–70. [PubMed: 18680557]
21. Weihofen WA, et al. , Crystal structure of CD26/dipeptidyl-peptidase IV in complex with adenosine deaminase reveals a highly amphiphilic interface. J Biol Chem, 2004. 279(41): p. 43330–5. [PubMed: 15213224]
22. Wang Z and Quiocho FA, Complexes of adenosine deaminase with two potent inhibitors: X-ray structures in four independent molecules at pH of maximum activity. Biochemistry, 1998. 37(23): p. 8314–24. [PubMed: 9622483]
23. O'Dwyer PJ, et al. , 2'-Deoxycoformycin (pentostatin) for lymphoid malignancies. Rational development of an active new drug. Ann Intern Med, 1988. 108(5): p. 733–43. [PubMed: 3282467]
24. Schaeffer HJ and Schwender CF, Enzyme inhibitors. 26. Bridging hydrophobic and hydrophilic regions on adenosine deaminase with some 9-(2-hydroxy-3-alkyl)adenines. J Med Chem, 1974. 17(1): p. 6–8. [PubMed: 4808472]
25. Richard E, et al. , The binding site of human adenosine deaminase for CD26/Dipeptidyl peptidase IV: the Arg142Gln mutation impairs binding to cd26 but does not cause immune deficiency. J Exp Med, 2000. 192(9): p. 1223–36. [PubMed: 11067872]
26. Gary E, et al. , Adenosine deaminase-1 enhances germinal center formation and functional antibody responses to HIV-1 Envelope DNA and protein vaccines. Vaccine, 2020. 38(22): p. 3821–3831. [PubMed: 32280045]
27. Chaffee S, et al. , IgG antibody response to polyethylene glycol-modified adenosine deaminase in patients with adenosine deaminase deficiency. J Clin Invest, 1992. 89(5): p. 1643–51. [PubMed: 1569204]
28. Dorsey MJ, et al. , PEGylated Recombinant Adenosine Deaminase Maintains Detoxification and Lymphocyte Counts in Patients with ADA-SCID. J Clin Immunol, 2023.
29. Hershfield MS, PEG-ADA replacement therapy for adenosine deaminase deficiency: an update after 8.5 years. Clin Immunol Immunopathol, 1995. 76(3 Pt 2): p. S228–32. [PubMed: 7554473]

Author Manuscript Author Manuscript Author Manuscript Author Manuscript

30. Schein CH, Production of Soluble Recombinant Proteins in Bacteria. Bio/Technology, 1989. 7(11): p. 1141–1149.
31. Shirano Y and Shibata D, Low temperature cultivation of Escherichia coli carrying a rice lipoxygenase L-2 cDNA produces a soluble and active enzyme at a high level. FEBS Lett, 1990. 271(1–2): p. 128–30. [PubMed: 2121525]
32. Schein CH and Noteborn MHM, Formation of Soluble Recombinant Proteins in Escherichia Coli is Favored by Lower Growth Temperature. Bio/Technology, 1988. 6(3): p. 291–294.
33. Chhetri G, Kalita P, and Tripathi T, An efficient protocol to enhance recombinant protein expression using ethanol in Escherichia coli. MethodsX, 2015. 2: p. 385–91. [PubMed: 26629417]
34. Rosano GL and Ceccarelli EA, Recombinant protein expression in Escherichia coli: advances and challenges. Front Microbiol, 2014. 5: p. 172. [PubMed: 24860555]
35. Rosano GL, Morales ES, and Ceccarelli EA, New tools for recombinant protein production in Escherichia coli: A 5-year update. Protein Sci, 2019. 28(8): p. 1412–1422. [PubMed: 31219641]
36. Porath J, et al. , Metal chelate affinity chromatography, a new approach to protein fractionation. Nature, 1975. 258(5536): p. 598–9. [PubMed: 1678]
37. Structural Genomics C, et al. , Protein production and purification. Nat Methods, 2008. 5(2): p. 135–46. [PubMed: 18235434]
38. Mohanty AK and Wiener MC, Membrane protein expression and production: effects of polyhistidine tag length and position. Protein Expr Purif, 2004. 33(2): p. 311–25. [PubMed: 14711520]
39. Gibson DG, Enzymatic assembly of overlapping DNA fragments. Methods Enzymol, 2011. 498: p. 349–61. [PubMed: 21601685]
40. Chazotte B, Labeling Golgi with fluorescent ceramides. Cold Spring Harbor Protocols, 2012. 2012(8): p. pdb. prot070599. [PubMed: 22854569]
41. Gracia E, et al. , The catalytic site structural gate of adenosine deaminase allosterically modulates ligand binding to adenosine receptors. FASEB J, 2013. 27(3): p. 1048–61. [PubMed: 23193172]
42. Kalckar HM, Differential spectrophotometry of purine compounds by means of specific enzymes; studies of the enzymes of purine metabolism. J Biol Chem, 1947. 167(2): p. 461–75. [PubMed: 20285041]
43. Lu J and Grenache DG, Development of a rapid, microplate-based kinetic assay for measuring adenosine deaminase activity in body fluids. Clin Chim Acta, 2012. 413(19–20): p. 1637–40. [PubMed: 22579767]
44. Tritsch GL, Validity of the continuous spectrophotometric assay of Kalckar for adenosine deaminase activity. Anal Biochem, 1983. 129(1): p. 207–9. [PubMed: 6859524]
45. Cercignani G and Allegrini S, On the validity of continuous spectrophotometric assays for adenosine deaminase activity: a critical reappraisal. Anal Biochem, 1991. 192(2): p. 312–5. [PubMed: 2035831]
46. Miroux B and Walker JE, Over-production of proteins in Escherichia coli: mutant hosts that allow synthesis of some membrane proteins and globular proteins at high levels. J Mol Biol, 1996. 260(3): p. 289–98. [PubMed: 8757792]
47. de Boer HA, Comstock LJ, and Vasser M, The tac promoter: a functional hybrid derived from the trp and lac promoters. Proc Natl Acad Sci U S A, 1983. 80(1): p. 21–5. [PubMed: 6337371]
48. Sunderhaus A, et al. , Comparative expression of soluble, active human kinases in specialized bacterial strains. PLoS One, 2022. 17(4): p. e0267226. [PubMed: 35439268]
49. Zhao D and Huang Z, Effect of His-Tag on Expression, Purification, and Structure of Zinc Finger Protein, ZNF191(243–368). Bioinorg Chem Appl, 2016. 2016: p. 8206854. [PubMed: 27524954]
50. Thomas JG and Baneyx F, Divergent effects of chaperone overexpression and ethanol supplementation on inclusion body formation in recombinant Escherichia coli. Protein Expr Purif, 1997. 11(3): p. 289–96. [PubMed: 9425634]
51. Kusano K, et al. , Protein synthesis inhibitors and ethanol selectively enhance heterologous expression of P450s and related proteins in Escherichia coli. Arch Biochem Biophys, 1999. 367(1): p. 129–36. [PubMed: 10375408]

Author Manuscript Author Manuscript Author Manuscript Author Manuscript

52. Rabhi-Essafi I, et al. , A strategy for high-level expression of soluble and functional human interferon α as a GST-fusion protein in E.coli. Protein Engineering, Design and Selection, 2007. 20(5): p. 201–209.
53. Dyson MR, et al. , Production of soluble mammalian proteins in Escherichia coli: identification of protein features that correlate with successful expression. BMC Biotechnology, 2004. 4(1): p. 32. [PubMed: 15598350]
54. Paraskevopoulou V and Falcone FH, Polyionic Tags as Enhancers of Protein Solubility in Recombinant Protein Expression. Microorganisms, 2018. 6(2).
55. Hochuli E, Purification of recombinant proteins with metal chelate adsorbent. Genet Eng (N Y), 1990. 12: p. 87–98. [PubMed: 1366709]
56. Janknecht R, et al. , Rapid and efficient purification of native histidine-tagged protein expressed by recombinant vaccinia virus. Proc Natl Acad Sci U S A, 1991. 88(20): p. 8972–6. [PubMed: 1924358]
57. Grisshammer R and Tucker J, Quantitative evaluation of neurotensin receptor purification by immobilized metal affinity chromatography. Protein Expr Purif, 1997. 11(1): p. 53–60. [PubMed: 9325139]
58. Khan F, He M, and Taussig MJ, Double-hexahistidine tag with high-affinity binding for protein immobilization, purification, and detection on ni-nitrilotriacetic acid surfaces. Anal Chem, 2006. 78(9): p. 3072–9. [PubMed: 16642995]
59. Wilkins MR, et al. , Protein identification and analysis tools in the ExPASy server. Methods Mol Biol, 1999. 112: p. 531–52. [PubMed: 10027275]
60. Akirov A, et al. , Low Albumin Levels Are Associated with Mortality Risk in Hospitalized Patients. Am J Med, 2017. 130(12): p. 1465 e11–1465 e19.
61. Krebs HA, Chemical composition of blood plasma and serum. Annu Rev Biochem, 1950. 19: p. 409–30. [PubMed: 14771836]
62. Robichon C, et al. , Engineering Escherichia coli BL21(DE3) derivative strains to minimize E. coli protein contamination after purification by immobilized metal affinity chromatography. Appl Environ Microbiol, 2011. 77(13): p. 4634–46. [PubMed: 21602383]
63. Andersen KR, Leksa NC, and Schwartz TU, Optimized E. coli expression strain LOBSTR eliminates common contaminants from His-tag purification. Proteins, 2013. 81(11): p. 1857–61. [PubMed: 23852738]
64. Mateo C, et al. , Affinity chromatography of polyhistidine tagged enzymes. New dextran-coated immobilized metal ion affinity chromatography matrices for prevention of undesired multipoint adsorptions. J Chromatogr A, 2001. 915(1–2): p. 97–106. [PubMed: 11358266]
65. Bolanos-Garcia VM and Davies OR, Structural analysis and classification of native proteins from E. coli commonly co-purified by immobilised metal affinity chromatography. Biochim Biophys Acta, 2006. 1760(9): p. 1304–13. [PubMed: 16814929]
66. Hirschhorn R, Yang DR, and Israni A, An Asp8Asn substitution results in the adenosine deaminase (ADA) genetic polymorphism (ADA 2 allozyme): occurrence on different chromosomal backgrounds and apparent intragenic crossover. Ann Hum Genet, 1994. 58(1): p. 1–9. [PubMed: 8031011]
67. Fanali G, et al. , Human serum albumin: from bench to bedside. Mol Aspects Med, 2012. 33(3): p. 209–90. [PubMed: 22230555]
68. Wilson DK and Quiocho FA, A pre-transition-state mimic of an enzyme: X-ray structure of adenosine deaminase with bound 1-deazaadenosine and zinc-activated water. Biochemistry, 1993. 32(7): p. 1689–94. [PubMed: 8439534]
69. Wilson DK, Rudolph FB, and Quiocho FA, Atomic structure of adenosine deaminase complexed with a transition-state analog: understanding catalysis and immunodeficiency mutations. Science, 1991. 252(5010): p. 1278–84. [PubMed: 1925539]
70. Sideraki V, et al. , Site-directed mutagenesis of histidine 238 in mouse adenosine deaminase: substitution of histidine 238 does not impede hydroxylate formation. Biochemistry, 1996. 35(47): p. 15019–28. [PubMed: 8942668]

Author Manuscript Author Manuscript Author Manuscript Author Manuscript

71. Kinoshita T, Tada T, and Nakanishi I, Conformational change of adenosine deaminase during ligand-exchange in a crystal. Biochem Biophys Res Commun, 2008. 373(1): p. 53–7. [PubMed: 18549808]

72. Kinoshita T, et al. , Structural basis of compound recognition by adenosine deaminase. Biochemistry, 2005. 44(31): p. 10562–9. [PubMed: 16060665]

73. Terasaka T, et al. , Structure-based design and synthesis of non-nucleoside, potent, and orally bioavailable adenosine deaminase inhibitors. J Med Chem, 2004. 47(11): p. 2728–31. [PubMed: 15139750]

74. Weihofen WA, et al. , Crystal structures of HIV-1 Tat-derived nonapeptides Tat-(1–9) and Trp2-Tat-(1–9) bound to the active site of dipeptidyl-peptidase IV (CD26). J Biol Chem, 2005. 280(15): p. 14911–7. [PubMed: 15695814]

75. Gentile C, et al. , Generation of a Retargeted Oncolytic Herpes Virus Encoding Adenosine Deaminase for Tumor Adenosine Clearance. Int J Mol Sci, 2021. 22(24).

76. Qu Y, et al. , Adenosine Deaminase 1 Overexpression Enhances the Antitumor Efficacy of Chimeric Antigen Receptor-Engineered T Cells. Hum Gene Ther, 2022. 33(5–6): p. 223–236. [PubMed: 34225478]

77. Wang L, et al. , Targeting Adenosine with Adenosine Deaminase 2 to Inhibit Growth of Solid Tumors. Cancer Res, 2021. 81(12): p. 3319–3332. [PubMed: 33863778]

78. Zhang C, et al. , Catalytical nano-immunocomplexes for remote-controlled sono-metabolic checkpoint trimodal cancer therapy. Nat Commun, 2022. 13(1): p. 3468. [PubMed: 35710545]

79. Zhao Z, et al. , An injectable hydrogel reshaping adenosinergic axis for cancer therapy. Advanced Functional Materials, 2022. 32(24): p. 2200801.

Author Manuscript Author Manuscript Author Manuscript Author Manuscript

Highlights:

- We detail how the use of a lysate-based activity screen to improve several expression conditions for production of human adenosine deaminase I (HsADA1) in *E. coli.*
- We demonstrate how engineering the affinity tag system can improve enzyme purity.
- Using our expression and purification platform, we characterize the properties of an HsADA1 variant with an Asp8Asn mutation
- We demonstrate that HsADA1 has an interesting property of being deactivated by exposure to human serum over time, despite having an initial albumin-driven increase in activity

Author Manuscript Author Manuscript Author Manuscript Author Manuscript

Highlights

- Development of a lysate-based assay to optimize recombinant expression of HsADA1.
- Double-histidine-tags enhance HsADA1 purity.
- Human adenosine deaminase activity is enhanced in human serum, partially by albumin.

Author Manuscript Author Manuscript Author Manuscript Author Manuscript

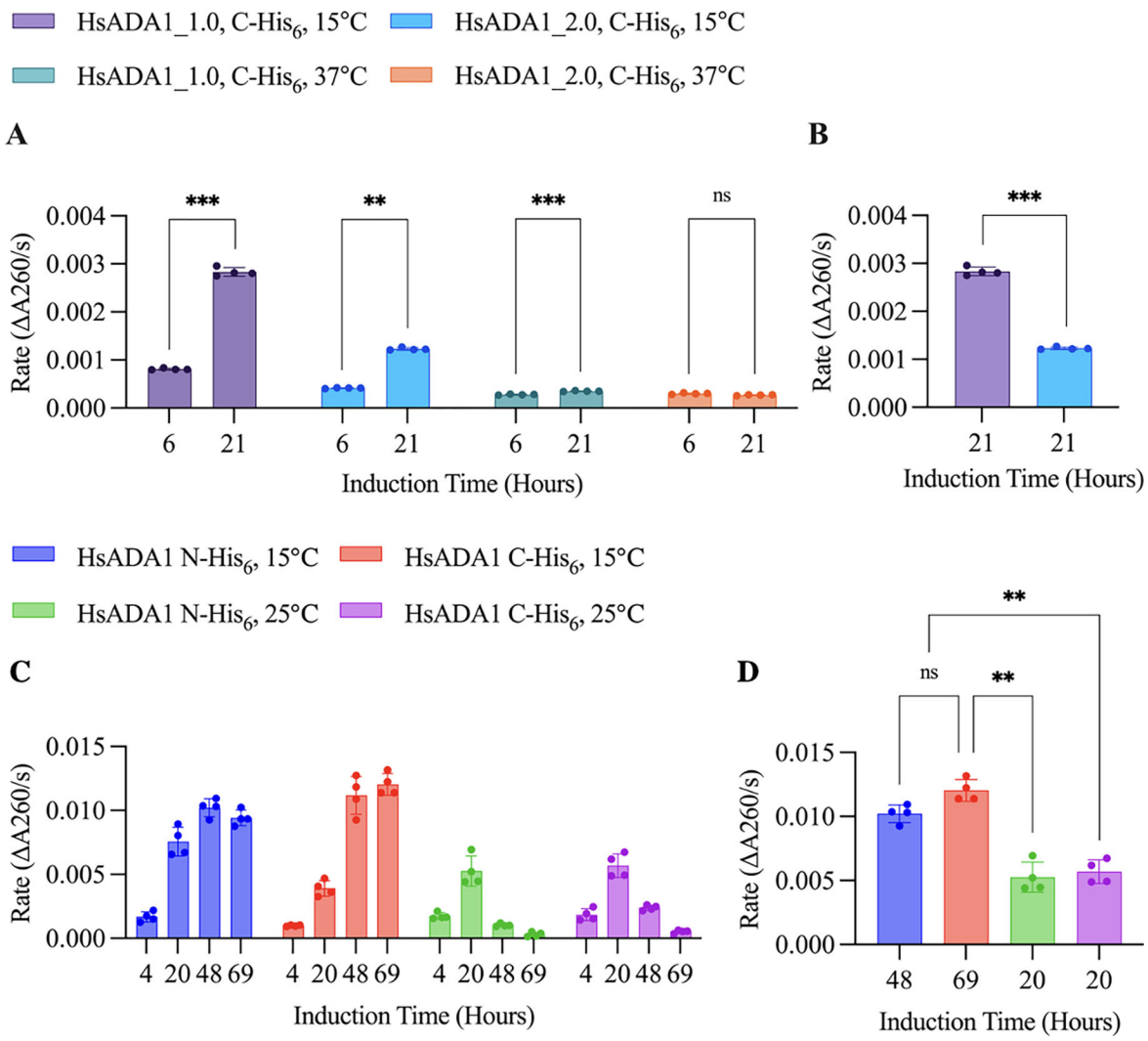

Figure 1.

HsADA1 activity in *E. coli* strain T7 Express lysate as a function of codon optimization, his-tag positioning induction temperature, and induction time (bars represent the mean ± standard deviation, n = 4 biological replicates, repeated measurement 3-way ANOVA). **(A)** Activity in the lysates of HsADA1_1.0 C-His$_6$ induced at 15°C (purple), HsADA1_2.0 C-His$_6$ induced at 15°C (blue), HsADA1_1.0 C-His$_6$ induced at 37°C (green), and HsADA1_2.0 C-His$_6$ induced at 37°C (orange) at the 6- and 21-hour measurements, respectively. **(B)** Maximum activity in the lysates of HsADA1_1.0 and HsADA1_2.0. ***p<0.01, ***p<0.001, ns = not significant.* **(C)** Activity in the lysates of HsADA1_1.0 N-His$_6$ induced at 15°C (blue), HsADA1_1.0 C-His$_6$ induced at 15°C (red), HsADA1_1.0 N-His$_6$ induced at 25°C (green), and HsADA1_1.0 C-His$_6$ induced at 25°C (purple) at the 4-, 20-, 48-, and 69-hour measurements **(D)** Comparison of the maximum activity in the lysates of HsADA1_1.0 C-His$_6$ and HsADA1_1.0 N-His$_6$ at 15°C and 25°C. ***p<0.01, ns = not significant.*

Author Manuscript Author Manuscript Author Manuscript Author Manuscript

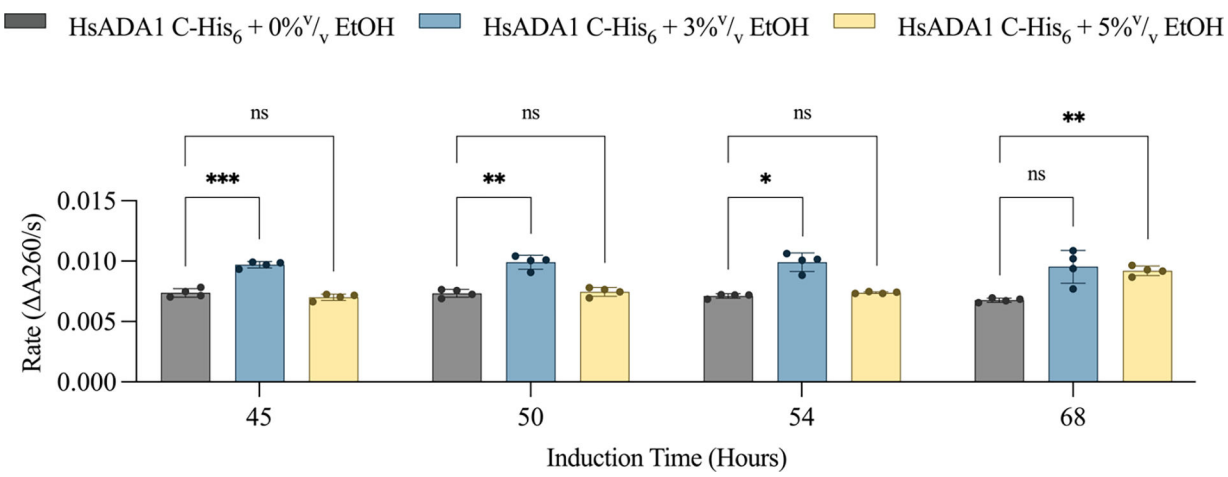

Figure 2.

HsADA1 activity in *E. coli* strain T7 Express lysate as a function of percent ethanol (EtOH) supplementation and induction time with the HsADA1_1.0 C-His_6 construct at 15°C (bars represent the mean ± standard deviation, n = 4 biological replicates, 2-way ANOVA). All comparisons between 0%$^{v}/_{v}$ EtOH (black) & 3%$^{v}/_{v}$ EtOH supplementation (blue) and 0%$^{v}/_{v}$ EtOH & 5%$^{v}/_{v}$ EtOH supplementation (yellow) are depicted. **p<0.05, **p<0.01, ** *p<0.001, ns = not significant.*

Author Manuscript Author Manuscript Author Manuscript Author Manuscript

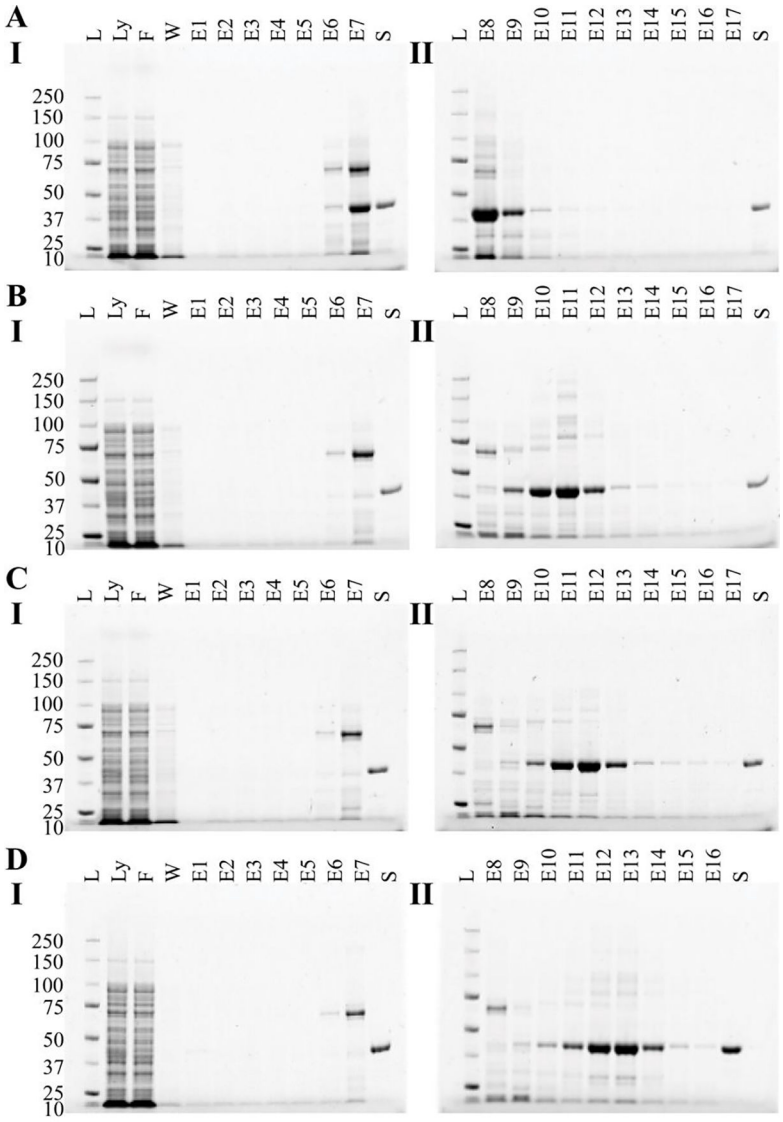

Figure 3.

Immobilized metal affinity chromatography (IMAC) elution time as a function of his-tag length for purifications from *E. coli* strain T7 Express harboring pET-28 a (+) HsADA1_1.0 plasmids. For each affinity purification, the lysate and wash buffer contained 20mM imidazole followed by a 20CV gradient elution from 20mM to 500mM imidazole. Each purification sequences spans two gels (**I** and **II**). Starting on **I** following the ladder (L), are lysate (Ly), IMAC column flow-through (F), IMAC wash (W), IMAC gradient elution fractions 1–7 (E1–7), and the final size exclusion chromatography (SEC) product of the pooled affinity fractions containing the HsADA1 product of interest (S). **II** begins with ladder (L), the remainder of the gradient elution fractions, and completes with the SEC product (S). IMAC and SEC purification sequence of HsADA1 C-His_6, C-His_6-His_6, C-His_6-His_8, and C-His_6-His_{10} correspond with panels **(A)**, **(B)**, **(C)**, and **(D)**, respectively. Full SDS-PAGE images are available in Supplementary Figure 6.

Author Manuscript Author Manuscript Author Manuscript Author Manuscript

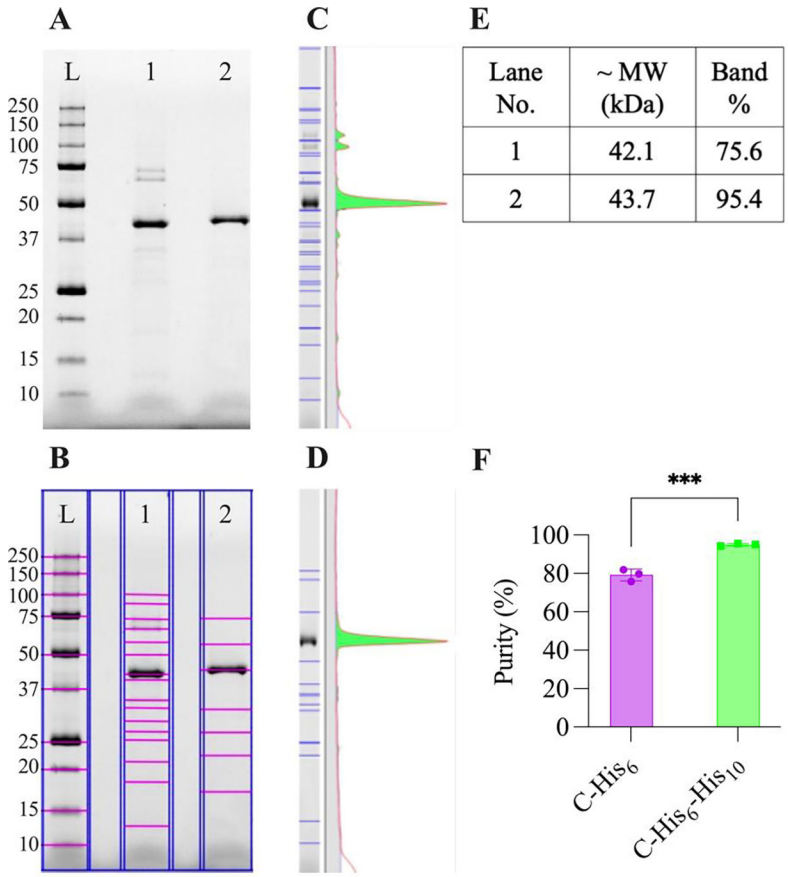

Fig. 4.

Size exclusion chromatography (SEC) product purity as determined by SDS-PAGE image analysis for purifications from E. coli strain T7 Express harboring pET-28 a (+) HsADA1_1.0 C-His6 or pET-28 a (+) HsADA1_1.0 CHis6-His10 plasmids. Image analysis was performed with Bio-Rad Image Lab software. (A) SDS-PAGE of ladder (L), HsADA1 C-His6 SEC product (1), and HsADA1 C-His6-His10 SEC product (2). (B) Band determination of the L, 1, and 2 lanes with pink lines signifying determined band locations. (C) Band volume analysis for lane 1 where a larger green peak denotes greater band volume. (D) Band volume analysis for lane 2. (E) Determination of HsADA1 product purity via band analysis for lanes 1 and 2. (F) HsADA1 C-His6 and C-His6-His10 SEC product purities determined via band analysis (bars represent the mean ± standard deviation n = 3 biological replicates each, two-tailed, unpaired t-test).

Author Manuscript Author Manuscript Author Manuscript Author Manuscript

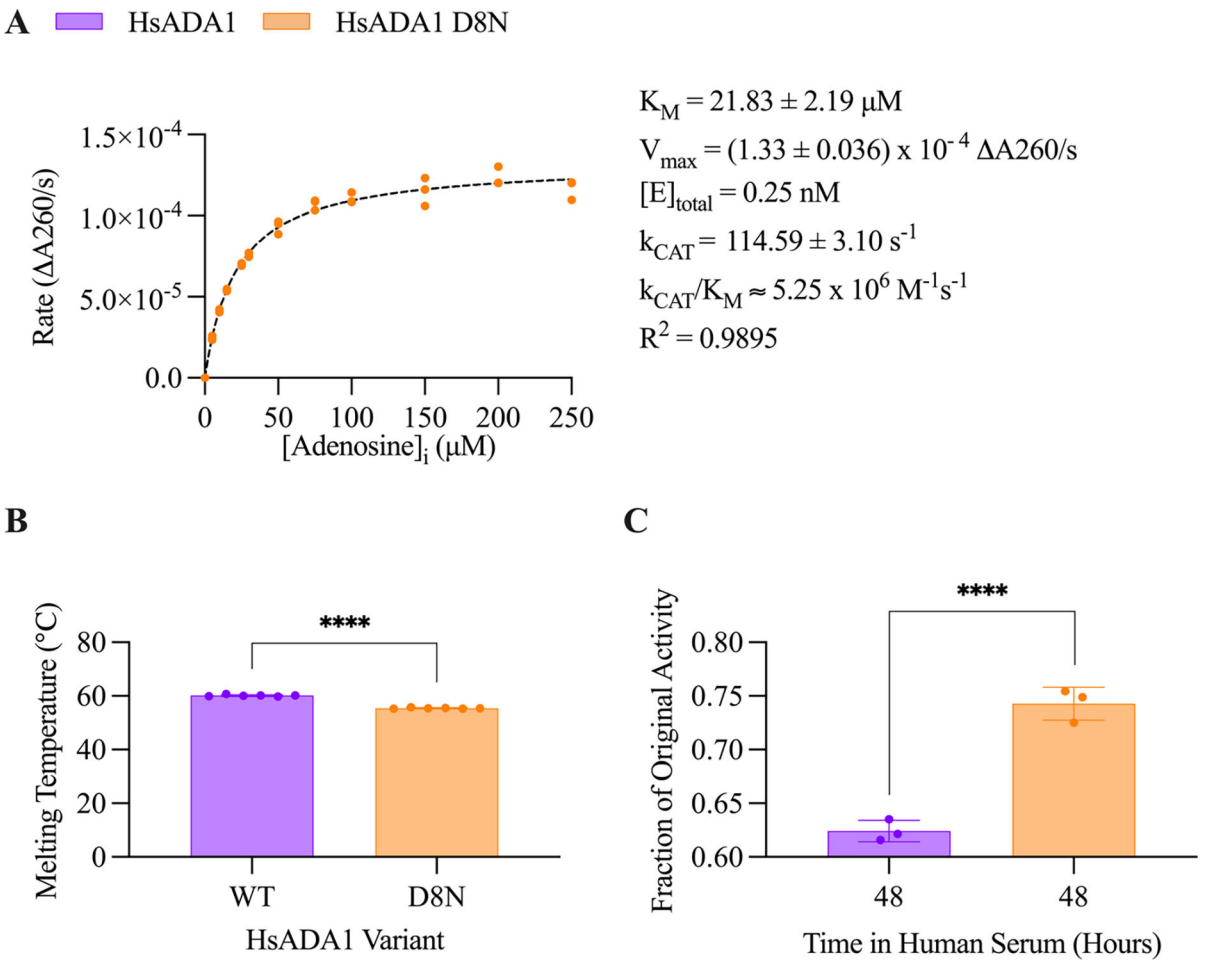

Figure 5.

Characterization of variant HsADA1 D8N (D8N) and select comparisons to wildtype (WT). All determinations were made in triplicate (n = 3) unless otherwise noted. **(A)** Nonlinear regression of the Michaelis-Menten equation to determine the kinetic parameters of HsADA1 D8N (orange). **(B)** Melting temperatures of wildtype HsADA1 versus that of HsADA1 D8N (purple and orange, respectfully) (bars represent the mean ± standard deviation, n = 6 sample replicates, two-tailed, unpaired t-test). **(C)** Wildtype HsADA1 versus HsADA1 D8N activity in human serum after 48 hours of incubation at 37°C (bars represent the mean ± standard deviation, 2-way ANOVA (WT vs D8N, 0 vs 48 hours)). *****p<0.0001.*

Author Manuscript Author Manuscript Author Manuscript Author Manuscript

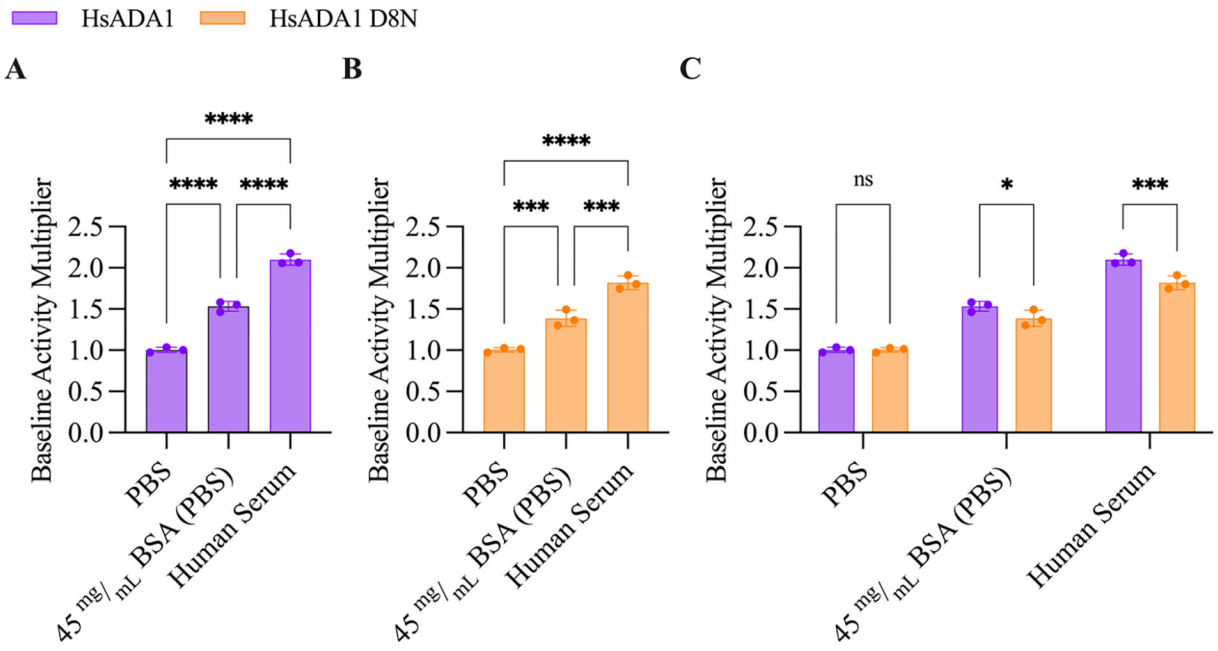

Figure 6.

The activity of wildtype HsADA1 and the D8N variant increase in the presence of bovine serum albumin (BSA) and human serum. All determinations were made in triplicate (n = 3). Normalized wildtype HsADA1 **(A)** or D8N variant **(B)** activity in the presence of 45mg/mL BSA (PBS) or human serum relative to baseline in PBS (bars represent the mean ± standard deviation, 1-way ANOVA). **(C)** Normalized wildtype HsADA1 versus the D8N variant's activity in the presence of BSA or human serum (bars represent the mean ± standard deviation, 2-way ANOVA). *ns = no significance*, **p<0.05*, ****p<0.001*, *****p<0.0001*.

Author Manuscript

Author Manuscript

Author Manuscript

Author Manuscript

Table 1

Physical properties of HsADA1 (wildtype) and HsADA1 D8N (D8N) with molecular weight (MW) in Daltons (Da), isoelectric point (pI), Michaelis-Menten constants (K_M, k_{CAT}, k_{CAT}/K_M), and melting temperature (T_m).

	MW (Da)*	pI (pH)*	K_M (μM)	k_{CAT} (s^{-1})	k_{CAT}/K_M ($M^{-1}s^{-1}$)	Tm (°C)
wildtype	40764.45	5.63	12.4 ± 1.60 [2]	94.6 ± 3.50 [2]	~7.62×10^6 [2]	60.1 ± 0.3
D8N	40800.39	5.39	21.83 ± 2.19	114.59 ± 3.10	~5.25×10^6	55.5 ± 0.2

* predicted with ExPASy ProtParam [59]